PHYSICAL REVIEW B VOLUME 56, NUMBER 10 1 SEPTEMBER 1997-II

Long-distance propagation and damping of low-frequency phonon polaritons in $LiNbO_3$

Tiequn Qiu and Max Maier
Naturwissenschaftliche Fakultät II-Physik, Universität Regensburg, D-93040 Regensburg, Germany
(Received 1 May 1997; revised manuscript received 27 June 1997)

The propagation and damping of low-frequency (10 to 80 cm^{-1}), picosecond phonon-polariton pulses have been investigated in $LiNbO_3$. The phonon polaritons propagate over a distance up to several centimeters. The measured frequency dependence of the absorption coefficient and the phase relaxation rate of the phonon polaritons is discussed using a model that takes into account the coupling of the phonon polaritons to a relaxational mode and to low-frequency excitations connected with defect centers. The much higher polariton damping at 300 K compared to 77 K is explained by the presence of the relaxational mode, which is missing at 77 K, and the larger coupling strength of the low-frequency excitations. The difference between the polariton damping of MgO doped $LiNbO_3$ and congruent $LiNbO_3$ is ascribed to the changes of the resonance frequencies of the defect centers. [S0163-1829(97)51534-7]

In recent years, the propagation and damping of phonon polaritons, which are of mixed mechanical and electromagnetic character, have attracted much attention.[1–9] Several techniques have been used to address the question of the dynamics and damping of phonon-polariton pulses. Impulsive stimulated Raman scattering and transient grating experiments with femtosecond laser pulses[1–5] have been used for investigations of ferroelectric crystals like $LiNbO_3$.[1,2] But these methods have the disadvantage that the frequency range of the investigated polaritons is limited from about 30 cm^{-1} to the linewidth of the femtosecond pulses of about 150 cm^{-1}. In addition, in crystals like $LiNbO_3$ measurements at temperatures substantially below room temperature are difficult, because the high intensity of the femtosecond laser pulses causes photorefractive damage.[4] Gain measurements of stimulated polariton scattering[6] can be used in principle for any polariton frequency, but for low frequencies (<80 cm^{-1} in $LiNbO_3$) the information on the damping of the polaritons is obscured by the effect of propagation of the polaritons out of the excitation region. In $LiNbO_3$ the dispersion curve of the polaritons of the 256-cm^{-1} A_1 phonon has been measured using femtosecond laser pulses,[1,2] and the damping of polaritons with frequencies larger than 80 cm^{-1} has been determined by gain measurements of stimulated polariton scattering.[6] The results have been discussed using a model where the polaritons are coupled to low-frequency excitations.[2,6]

The propagation and damping of polaritons has also been studied using a nonlocal time-delayed coherent anti-Stokes Raman scattering (CARS) technique in NH_4Cl and $LiIO_3$ crystals.[7–9] Polaritons with frequencies larger than 600 cm^{-1} have been investigated and propagation distances of the order of 1 mm and phase relaxation rates in the range from 0.1 to 1 ps^{-1} have been observed.

In this paper, we apply the nonlocal time-delayed CARS technique to the investigation of phonon polaritons of the 256-cm^{-1} A_1 mode of doped and undoped $LiNbO_3$ crystals and present information on the propagation and damping of low-frequency polaritons (10 to 80 cm^{-1}). It was found in $LiNbO_3$ that, even at room temperature, there is a coupling of the polaritons to a Debye relaxational mode, which provides an important contribution to the polariton damping. The existence of the relaxational mode has been taken as evidence that the ferroelectric phase transition is of order-disorder character or mixed displacive–order-disorder character.[10,11] A second important contribution to the polariton damping is the coupling of the polaritons to low-frequency excitations, which we suggest to be related to defect centers. The polariton damping at liquid nitrogen temperature is substantially smaller than at room temperature due to the vanishing of the relaxational mode and the smaller coupling strength of the low-frequency excitations. The difference between the polariton damping in MgO doped $LiNbO_3$ and undoped congruent $LiNbO_3$ is explained by the different resonance frequencies of the defect centers in these crystals.

Polariton pulses with a wave number $\overline{\nu}=\overline{\nu_L}-\overline{\nu_S}$ and a wave vector $\mathbf{k}=\mathbf{k}_L-\mathbf{k}_S$ are excited by superimposing in the lithium niobate crystal a pump laser beam (subscript L) and a Stokes beam (subscript S), which are linearly polarized parallel to the c axis of the crystal, under the phase matching angle θ (see Fig. 1). In order to limit the spatial extension of the polariton excitation region to a small size, the crystal was cut at one corner (see Fig. 1, right). The cut was filled with an absorbing layer which blocks the pump laser and Stokes

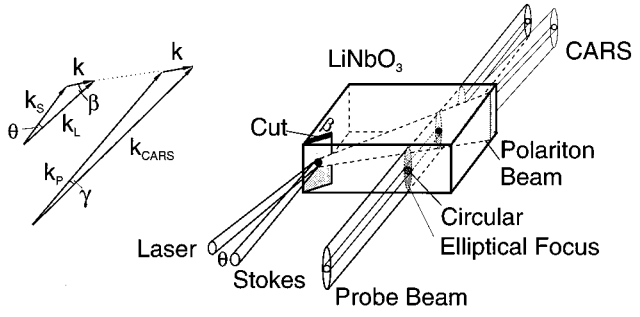

FIG. 1. Generation and detection of phonon polaritons in $LiNbO_3$. Left: Phase-matching diagrams; $\mathbf{k}$, $\mathbf{k}_S$, $\mathbf{k}_L$, $\mathbf{k}_P$, and $\mathbf{k}_{CARS}$ are the wave vectors of the polariton, Stokes, laser, probe and CARS waves. Right: Schematic diagram of the central part of the experimental setup.

beams. The pump laser and Stokes beams are provided by the fundamental of a mode-locked Nd:YAG laser and the idler of an optical parametric oscillator, which is synchronously pumped by the third harmonic of the Nd:YAG laser pulse train. For the polariton generation a single pulse is selected from the pump laser pulse train by a pulse slicer. The pulse durations of the pump laser and Stokes pulses are 35 and 28 ps, respectively. The linewidth of the idler light, which was continuously tunable around the fundamental wavelength of the pump laser of 1.064 μm, was about 1 cm^{-1}. The wave number of the generated polaritons was tuned by changing the idler wave number and adjusting the phase matching angle θ.

The excited polariton pulse propagates in the isotropic plane of the crystal with the group velocity v_G (Ref. 12) in the direction of its wave vector $\mathbf{k}$, which forms an angle $\beta \approx 65°$ with respect to the wave vector $\mathbf{k}_L$ of the pump laser beam (see Fig. 1, left). The polaritons are detected after propagating a distance X in the $LiNbO_3$ crystal by time-delayed, properly phase-matched CARS of a probe pulse (subscript P), which is selected by a pulse slicer from the second harmonic of the pump laser pulse train. Partial separation of the probe and CARS beams, which propagate in slightly different directions because of the fulfillment of the phase-matching condition, is achieved by a slit, which transmits mainly the CARS beam. Since for low-frequency polaritons the phase matching angle γ is very small (see Fig. 1, left) and the spatial discrimination is not complete, the CARS beam is directed on the entrance slit of a double monochromator and detected at the exit slit with a photomultiplier.

The laser and Stokes beams, which generate the polaritons, were focused to a cylindrical focal volume with a length l of 1.5 mm and a 1/e radius r_0 of 250 μm, which is of the order of the wavelength of 200 μm (in the crystal) of the lowest-frequency polaritons (10 cm^{-1}). Because of the large horizontal extension l of the interaction region of the laser and Stokes beams the horizontal divergence should be small. In contrast, the small focal spot radius r_0 is expected to cause a large divergence of the polariton beam in the vertical direction. We measured the radial energy distribution of the polariton beam by scanning a circularly focused probe beam (1/e radius $r_P = 180$ μm) in the vertical direction and detecting the generated CARS signal (Fig. 1, right). From the radial profile the 1/e radius r of the polariton beam was determined. In Fig. 2(a) the radius r is plotted versus propagation distance X of the polaritons for different polariton wave numbers $\bar{\nu}$ at liquid nitrogen temperature. The curves have been calculated by fitting hyperbolas to the experimental points. The divergence angle of the polariton beam is equal to the angle between the asymptote of the hyperbola and the X axis. It increases proportional to the polariton wavelength $\lambda \propto 1/\bar{\nu}$. For all polariton wavelengths the divergence angle is larger by a factor of 3 than that of a diffraction limited beam. It follows from these results that for the measurement of the polariton damping we have to use a probe beam which covers the complete polariton beam. This is achieved by focusing the probe beam with a cylindrical lens to an elliptical spot with the large axis in the vertical direction (see Fig. 1, right).

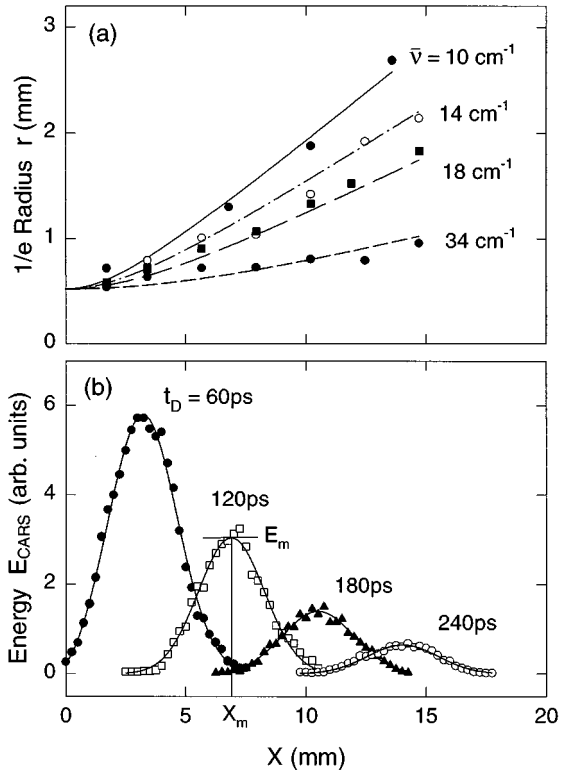

FIG. 2. (a) Radius r of the polariton beam versus propagation distance X for different polariton wave numbers $\bar{\nu}$ (liquid nitrogen temperature). (b) CARS energy E_{CARS} of the 12-cm^{-1} polariton versus propagation distance X for several delay times t_D (room temperature). X_m and E_m represent the position and height of the maximum of a polariton pulse, respectively.

We have measured the CARS energy E_{CARS} for a definite delay time t_D of the probe pulse at different positions X of the probe beam in the crystal. This corresponds to a snapshot of the polariton pulse. Figure 2(b) shows several snapshots at different delay times t_D, which demonstrate the propagation of the polariton pulse with a wave number of 12 cm^{-1} over a distance of about 1.5 cm at room temperature. In the figure, the CARS energy E_{CARS} is plotted versus position X of the probe beam in the polariton propagation direction for different delay times t_D. The solid curves represent a fit of Gaussian curves through the experimental points. The group velocity v_G of the polariton pulse was obtained from the position X_m of the pulse maximum at different delay times t_D. The absorption coefficient α and the phase relaxation time T_2 were determined from the plot of the logarithm of the height E_m of the polariton pulse maximum versus position X_m and delay time t_D, respectively. We obtained a group velocity of $v_G = 0.20 \times c$, where c is the vacuum light velocity, an absorption coefficient of $\alpha = 1.9$ cm^{-1}, and a phase relaxation time of $T_2 = 170$ ps for the 12-cm^{-1} polariton at room temperature. Since the polariton pulse propagates with the group velocity v_G, the spatial and the temporal damping constants are related by $\alpha = 2/(v_G T_2)$.[8]

We have determined the group velocity v_G, the absorption coefficient α, and the phase relaxation time T_2 in the way described above for polariton pulses with wave numbers between 10 and 80 cm^{-1} in congruent $LiNbO_3$ and MgO

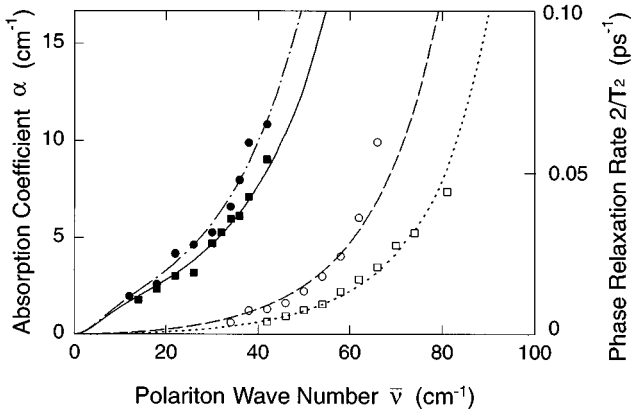

FIG. 3. Absorption coefficient α (left-hand scale) and phase relaxation rate $2/T_2$ (right-hand scale) versus phonon-polariton wave number $\overline{\nu}$ for MgO:$LiNbO_3$ (squares) and congruent $LiNbO_3$ (circles) at $T=77$ K (open symbols) and 300 K (full symbols). The curves have been calculated with Eqs. (1) to (4) using the following values. $\epsilon_\infty=8.31$, MgO:$LiNbO_3$, $T=77$ K (dotted curve), $S_0=16.1$, $\overline{\nu_1}=115\ \mathrm{cm}^{-1}$, $\delta\overline{\nu_1}=30\ \mathrm{cm}^{-1}$, $K_1=5.06\times10^6\ \mathrm{cm}^{-4}$, $\Delta=0\ \mathrm{cm}^{-1}$; $T=300$ K (solid curve), $S_0=16.3$, $\overline{\nu_1}=115\ \mathrm{cm}^{-1}$, $\delta\overline{\nu_1}=45\ \mathrm{cm}^{-1}$, $K_1=30.25\times10^6\ \mathrm{cm}^{-4}$, $\Delta=26\ \mathrm{cm}^{-1}$, $\tau=0.6$ ps; congruent $LiNbO_3$, $T=77$ K (dashed curve), $S_0=17.6$, $\overline{\nu_1}=105\ \mathrm{cm}^{-1}$, $\delta\overline{\nu_1}=40\ \mathrm{cm}^{-1}$, $K_1=4.92\times10^6\ \mathrm{cm}^{-4}$, $\overline{\nu_2}=120\ \mathrm{cm}^{-1}$, $\delta\overline{\nu_2}=15\ \mathrm{cm}^{-1}$, $K_2=1.10\times10^6\ \mathrm{cm}^{-4}$, $\Delta=0\ \mathrm{cm}^{-1}$; $T=300$ K (dash-dotted curve), $S_0=17.8$, $\overline{\nu_1}=105\ \mathrm{cm}^{-1}$, $\delta\overline{\nu_1}=40\ \mathrm{cm}^{-1}$, $K_1=27.26\times10^6\ \mathrm{cm}^{-4}$, $\overline{\nu_2}=120\ \mathrm{cm}^{-1}$, $\delta\overline{\nu_2}=15\ \mathrm{cm}^{-1}$, $K_2=6.12\times10^6\ \mathrm{cm}^{-4}$, $\Delta=26\ \mathrm{cm}^{-1}$, $\tau=0.6$ ps.

doped $LiNbO_3$ at room temperature and liquid nitrogen temperature (77 K). The absorption coefficient α (left-hand scale) and the phase relaxation rate $2/T_2$ (right-hand scale) are plotted versus polariton wave number $\overline{\nu}$ in Fig. 3. Two main results can be seen from the figure. (i) The absorption coefficient of congruent $LiNbO_3$ (circles) is larger than that of MgO:$LiNbO_3$ (squares). (ii) The absorption at 77 K (open symbols) is substantially smaller than at 300 K (full symbols). These results will be discussed in the following.

The damping of the polaritons is determined by the dielectric function $\epsilon(\overline{\nu})$. The absorption coefficient α is given by[13]

$$\alpha=4\pi\overline{\nu}\overline{n}'', \tag{1}$$

where n'' is the imaginary part of the refractive index. It is related to the real and imaginary parts, ϵ' and ϵ'', of the dielectric function by

$$n''=\left\{\frac{1}{2}\left[(\epsilon'^2+\epsilon''^2)^{1/2}-\epsilon'\right]\right\}^{1/2}. \tag{2}$$

For a single polar phonon mode model with an eigenfrequency $\overline{\nu_0}$ (256 cm^{-1} in $LiNbO_3$) the dielectric function can be written as

$$\epsilon(\overline{\nu})=\epsilon_\infty+\frac{S_0\overline{\nu_0^2}}{\overline{\nu_0^2}-\overline{\nu^2}-i\overline{\nu}\delta\overline{\nu_0}}. \tag{3}$$

Here, S_0 and $\delta\overline{\nu_0}$ are the oscillator strength and damping constant, respectively, of the phonon mode. However, it has been shown[2,4,6] that this simple model cannot describe correctly the dispersion relation and damping of the polaritons. It has been extended in two different ways: first, by coupling low-frequency excitations to the mechanical part of the polariton[4,6] and, second, by assuming that these excitations have oscillator strengths providing a coupling to the light field.[2] In the first model the mode coupling increases the damping of the polaritons. It can be described by replacing $\delta\overline{\nu_0}$ in Eq. (3) by an effective damping constant[6]

$$\delta\overline{\nu_{eff}}=\delta\overline{\nu_0}+\frac{1}{i\overline{\nu}}\sum_j\frac{K_j}{\overline{\nu_j^2}-\overline{\nu^2}-i\overline{\nu}\delta\overline{\nu_j}}. \tag{4}$$

Here, $\overline{\nu_j}$ and $\delta\overline{\nu_j}$ are the eigenfrequency and damping constant of the low-frequency excitation j, and K_j represents the coupling constant of the mechanical part of the polariton to this excitation. In the second model,[2] where oscillator strengths are ascribed to the low-frequency excitations, further resonance terms are added to the dielectric constant ϵ [right hand side of Eq. (3)], which take into account the coupling of the excitations to the light field. We found that our experimental results can be described within the experimental accuracy by both models. In the following we discuss for simplicity only the coupling of low-frequency excitations to the mechanical part of the polariton.

Information on the low-frequency excitations can also be obtained from spontaneous Raman spectra. We have measured the spontaneous Raman spectra of the crystals used in our experiments for a scattering angle of 90°. In the region below 150 cm^{-1} a very weak and broad Raman peak was observed in MgO:$LiNbO_3$ at 115 cm^{-1}, which splitted into two overlapping peaks at 105 and 120 cm^{-1} in congruent $LiNbO_3$. The frequencies of these peaks are significantly smaller than that of the lowest-frequency optical phonon mode of $LiNbO_3$ (E mode at 152 cm^{-1}). In addition, they depend on the composition of the crystal. We ascribe therefore these low-frequency resonances to defect centers in the crystal. They may be caused by vibrational defect modes or electronic traps in $LiNbO_3$.[14] The resonance frequencies of the low-frequency excitations in congruent and MgO-doped $LiNbO_3$ have also been determined in Refs. 2, 6, and 15. The resonance frequency $\overline{\nu_1}=115\ \mathrm{cm}^{-1}$ in MgO:$LiNbO_3$ measured by us is consistent within the experimental accuracy with the result of Ref. 6 (about 120 cm^{-1}). In congruent $LiNbO_3$ our values of 105 and 120 cm^{-1} for the resonance frequencies of the defect centers do not agree with those of Ref. 2 and 15. The reason for this difference is not clear at present.

For the calculation of the absorption coefficient α we have to know the damping constant $\delta\overline{\nu_0}$ in Eq. (4). In Ref. 6 a model has been introduced in which $\delta\overline{\nu_0}$ is determined by the decay of the phonon part of the polariton into two acoustic phonons and the scattering of the polaritons at crystal imperfections. This model leads to a dependence of the damping constant $\delta\overline{\nu_0}$ on the polariton frequency $\overline{\nu}$.

Using the results of Ref. 6 [Eq. (4)] for $\delta\overline{\nu_0}$ and the resonance frequencies $\overline{\nu_j}$ and the linewidths $\delta\overline{\nu_j}$ of the defect centers from our spontaneous Raman measurements, the only fit parameters are the coupling constants K_j in Eq. (4). We calculated the absorption coefficient α for congruent and MgO-doped $LiNbO_3$ at 77 K as a function of polariton wave number $\overline{\nu}$ using Eqs. (1)–(4). The results are shown as

dashed and dotted lines for congruent and MgO doped $LiNbO_3$, respectively, in Fig. 3. There is good agreement between the experimental points and the calculated curves. The larger absorption coefficient of congruent $LiNbO_3$ is mainly due to the down shift of the resonance frequency ($105\ cm^{-1}$) of the defect center compared to MgO:$LiNbO_3$ ($115\ cm^{-1}$). The wing of this mode causes the larger absorption.

For the fit of the experimental data at room temperature we took into account that the broad peaks in the spontaneous Raman spectrum became stronger by a factor of 2 when the temperature was raised from 77 to 300 K. But the corresponding calculated absorption coefficient was smaller than the measured values. By increasing the coupling strength K_j of the low-frequency excitations it was not possible to account quantitatively for the measured frequency dependence of the polariton absorption coefficient. The reason is that the wings of the low-frequency resonances cause a nearly quadratic frequency dependence of the absorption coefficient in the low-frequency region ($\overline{\nu} \leqslant 30\ cm^{-1}$ at $T=300$ K), while the measured absorption coefficient rises nearly linearly in this frequency region. Consequently it was not possible to describe the experimental results just by coupling to the low-frequency excitations.

Since there was evidence from our spontaneous Raman spectra that there is a coupling of the phonon mode to a Debye relaxational mode at room temperature, we added to the effective damping constant in Eq. (4) a term of the form[10,11]

$$\delta\overline{\nu_D} = \frac{1}{i\overline{\nu}} \frac{\Delta^2}{1 - i2\pi c\overline{\nu}\tau}, \tag{5}$$

where τ is the relaxation time and Δ is the coupling parameter. When this term is included, good agreement is obtained in Fig. 3 between the room temperature experiments (filled symbols) and the calculations (solid and dash-dotted curves) for values of $\tau = 0.6$ ps and $\Delta = 26\ cm^{-1}$. This result clearly shows that the coupling of the polaritons to a relaxational mode provides an important contribution to the absorption coefficient at room temperature. This shows clear evidence for the existence of a relaxational mode at *room temperature* is found in $LiNbO_3$. The relaxational mode was taken as evidence that the ferroelectric phase transition is of order-disorder character or mixed displacive–order-disorder character.[10,11] In a previous investigation[10] the values for the relaxation time τ and the coupling parameter Δ of the relaxational mode have been determined at temperatures higher than 600 K for congruent and stoichiometric $LiNbO_3$. In congruent $LiNbO_3$ a temperature-independent value[16] of $\tau = 0.3$ ps was found between 612 and 1224 K. It was suggested,[10] that the defect concentration limits the relaxation time τ in congruent $LiNbO_3$. The value of Δ ($=65\ cm^{-1}$ at 612 K) was temperature dependent. An extrapolation to room temperature using Fig. 6 of Ref. 10 gives a value of the coupling parameter of $\Delta = 52\ cm^{-1}$. The values for τ and Δ of this work and Ref. 10 are of the same order of magnitude. The difference of about a factor of 2 may be due to the different temperature ranges of the measurements and the extrapolation of the high-temperature data to room temperature. Moreover, the congruent $LiNbO_3$ crystals may differ by the types and concentrations of defect centers because the crystal suppliers may use different crystal growing conditions.

In conclusion, long-distance propagation up to several centimeters of low-frequency polaritons has been observed in congruent $LiNbO_3$ and MgO doped $LiNbO_3$. The damping of the polaritons has been discussed in terms of the polariton coupling to a relaxational mode and to low-frequency excitations connected with defect centers. The relaxational mode provides an important contribution to the polariton damping at 300 K.

The authors gratefully acknowledge financial support by the Deutsche Forschungsgemeinschaft. We thank U. T. Schwarz for valuable discussions and a critical reading of the manuscript.

[1] P. C. M. Planken, L. D. Noordam, J. T. M. Kennis, and A. Lagendijk, Phys. Rev. B **45**, 7106 (1992).

[2] H. J. Bakker, S. Hunsche, and H. Kurz, Phys. Rev. B **50**, 914 (1994).

[3] H. J. Bakker, S. Hunsche, and H. Kurz, Phys. Rev. B **48**, 13 524 (1993).

[4] G. P. Wiederrecht, T. P. Dougherty, L. Dhar, K. A. Nelson, D. E. Leaird, and A. M. Weiner, Phys. Rev. B **51**, 916 (1995).

[5] H. M. Perry and T. P. Dougherty, Phys. Rev. B **55**, 5778 (1997).

[6] U. T. Schwarz and M. Maier, Phys. Rev. B **53**, 5074 (1996).

[7] G. M. Gale, F. Vallée, and C. Flytzanis, Phys. Rev. Lett. **57**, 1867 (1986).

[8] F. Vallée and C. Flytzanis, Phys. Rev. B **46**, 13 799 (1992).

[9] F. Vallée and C. Flytzanis, Phys. Rev. Lett. **74**, 3281 (1995).

[10] Y. Okamoto, P.-C. Wang, and J. F. Scott, Phys. Rev. B **32**, 6787 (1985).

[11] M.-S. Zhang and J. F. Scott, Phys. Rev. B **34**, 1880 (1986).

[12] In Ref. 13 the energy velocity is used instead of the group velocity. However, in our case the difference between both velocities is negligible.

[13] R. Loudon, J. Phys. A **3**, 233 (1970).

[14] O. F. Schirmer, H.-J. Reyher, and M. Wöhlecke, in *Insulating Materials for Optoelectronics*, edited by F. Aguilló López (World Scientific, Singapore, 1995), Chap. 4; K. L. Sweeney, L. E. Halliburton, D. A. Bryan, R. R. Rice, R. Gerson, and H. E. Tomaschke, J. Appl. Phys. **57**, 1036 (1985).

[15] T. Qiu, T. Tillert, and M. Maier, Opt. Commun. **19**, 149 (1995).

[16] The values for the relaxation times τ given in Refs. 10 and 11 refer to the frequency ν (or wave number $\overline{\nu}$), not to the circular frequency ω. They are related to the relaxation times of this work by τ (this work) $= \tau$ (Refs. 10, 11)/(2π).